Sheffield Hallam University

Energy and exergy analysis of chemical looping combustion technology and comparison with pre-combustion and oxy-fuel combustion technologies for CO2 capture

MUKHERJEE, Sanjay, KUMAR, Prashant, YANG, Aidong and FENNEL, Paul

Published version

MUKHERJEE, Sanjay, KUMAR, Prashant, YANG, Aidong and FENNEL, Paul (2015). Energy and exergy analysis of chemical looping combustion technology and comparison with pre-combustion and oxy-fuel combustion technologies for CO2 capture. Journal of Environmental Chemical Engineering, 3 (3), 2104-2114.

Repository use policy

Energy and exergy analysis of chemical looping combustion technology and comparison with pre-combustion and oxy-fuel combustion technologies for CO_2 capture

Sanjay Mukherjee[a], Prashant Kumar[a,*], Aidong Yang[b], Paul Fennell[c]

[a] Department of Civil and Environmental Engineering, University of Surrey, Guildford, Surrey GU2 7XH, United Kingdom
[b] Department of Engineering Science, University of Oxford, Parks Road, Oxford OX1 3PJ, United Kingdom
[c] Department of Chemical Engineering, Imperial College London, South Kensington, London SW7 2AZ, United Kingdom

ABSTRACT

Carbon dioxide (CO_2) emitted from conventional coal-based power plants is a growing concern for the environment. Chemical looping combustion (CLC), pre-combustion and oxy-fuel combustion are promising CO_2 capture technologies which allow clean electricity generation from coal in an integrated gasification combined cycle (IGCC) power plant. This work compares the characteristics of the above three capture technologies to those of a conventional IGCC plant without CO_2 capture. CLC technology is also investigated for two different process configurations—(i) an integrated gasification combined cycle coupled with chemical looping combustion (IGCC–CLC), and (ii) coal direct chemical looping combustion (CDCLC)—using exergy analysis to exploit the complete potential of CLC. Power output, net electrical efficiency and CO_2 capture efficiency are the key parameters investigated for the assessment. Flowsheet models of five different types of IGCC power plants, (four with and one without CO_2 capture), were developed in the Aspen plus simulation package. The results indicate that with respect to conventional IGCC power plant, IGCC–CLC exhibited an energy penalty of 4.5%, compared with 7.1% and 9.1% for pre-combustion and oxy-fuel combustion technologies, respectively. IGCC–CLC and oxy-fuel combustion technologies achieved an overall CO_2 capture rate of $\sim$100% whereas pre-combustion technology could capture $\sim$94.8%. Modification of IGCC–CLC into CDCLC tends to increase the net electrical efficiency by 4.7% while maintaining 100% CO_2 capture rate. A detailed exergy analysis performed on the two CLC process configurations (IGCC–CLC and CDCLC) and conventional IGCC process demonstrates that CLC technology can be thermodynamically as efficient as a conventional IGCC process.

Introduction

Combustion of carbonaceous fuels (mainly coal, which is cheap and widely available) to produce electricity in power plants emits CO_2, which causes climate change [1]. Coal will continue to dominate power production in the near future due to its lower price and 113 years of reserves globally [2,3], although it is highly polluting [4]. Therefore, developing clean and cheap energy from coal has been an issue of international concern and a challenge for engineers and researchers [5]. Substantial efforts are being made worldwide to find new technologies to use coal in an environmentally-friendly manner [6–9].

Integrated gasification combined cycle coupled with chemical looping combustion (IGCC–CLC) and direct coal chemical looping combustion (CDCLC) are promising technologies to produce clean electricity from coal by efficiently incorporating CO_2 capture [10–14]. Chemical looping combustion (CLC) systems consist of two interconnected fluidised bed reactors which separately effect the oxidation and reduction reactions of an oxygen carrier (OC) [15,16]. The OC particles are continuously circulated to supply oxygen for combustion of solid or gaseous fuel(s). This arrangement prevents dilution of products of combustion (steam and CO_2) with nitrogen (N_2). Steam is condensed out, to obtain a pure stream of CO_2 for

transport and storage. Cormos [11] and Erlach et al. [12] presented a detailed plant concept and methodology for an IGCC–CLC process which would exhibit a net electrical efficiency of 39% and a CO_2 capture rate of ∼100%. Cormos and Cormos [10] evaluated thoroughly plant configuration and operational aspects for CDCLC processes. Their study showed that CDCLC can achieve a net electrical efficiency of 42.01% with a 99.81% CO_2 capture rate.

Physical absorption-based pre-combustion capture, and capture following oxy-fuel combustion, are another two promising technologies for CO_2 capture, which are commonly studied [17–20]. Oxy-fuel combustion involves burning the fuel in a mixture of pure oxygen and recycled CO_2 (the CO_2 serves as thermal ballast, to reduce the overall flame temperature, which would be exceedingly high for a mixture of pure oxygen and fuel). Pre-combustion capture includes the gasification of the fuel, which involves reaction with oxygen in sub-stoichiometric quantities to produce a mixture of carbon monoxide (CO), CO_2, methane (CH_4), hydrogen (H_2) and steam/vapour (H_2O). The CH_4 from the gasification is subsequently reformed in the presence of steam to a mixture of CO and H_2, and finally the CO undergoes the water–gas shift reaction with H_2O to produce a mixture of CO_2 and H_2, with the CO_2 being removed and the H_2 then burned in a modified gas turbine or used to power a fuel cell (after significant clean-up). Chiesa et al. [18] investigated physical absorption-based (Selexol solvent) pre-combustion capture for an IGCC plant producing 390–425 MW electricity. They observed a net electrical efficiency between 36 and 39% with ∼91% CO_2 capture rate and a 6.1–7.5% efficiency penalty against reference cases without CO_2 capture. Padurean et al. [60] compared different types of physical (Selexol, Rectisol, Purisol) and chemical (MDEA) solvents by applying physical absorption-based pre-combustion capture technologies to a base-case IGCC plant with 425–450 MW power output. They concluded that the IGCC process using Selexol is the most efficient capture technology, with a net electrical output of 36.08% and a CO_2 capture rate of 91.43%. A collaborative project between Vattenfall Group, Energy Research Centre of the Netherlands and Delft University of Technology has successfully developed and validated methodology and tool for retrofitting a Selexol based pre-combustion capture method for an IGCC plant at Groningen, Netherlands [21].

Studies on oxy-fuel combustion are mainly restricted to pulverised coal (PC) power plants. However, some studies have proposed new process designs to incorporate oxy-fuel combustion into IGCC plants. For instance, Oki et al. [20] demonstrated an innovative oxy-fuel IGCC process using pure oxygen instead of air in the gas turbine (GT) combustor unit of an IGCC. This configuration prevents dilution of the GT exhaust stream with N_2 and produces a pure CO_2 stream. Experimental apparatus constructed for their new oxy-fuel IGCC process was used to test the performance of different types of fuels (coal and biomass) for power generation. Kunze and Spliethoff [19] have also proposed an advanced process design, using combination IGCC and oxy-fuel combustion technologies that purports a net electrical efficiency of 45.74% and is capable of capturing 96–99% CO_2. Supplementary information (SI) Table S1 shows a comparison of different CO_2 capture technologies through published literature.

Existing work discussing individual capture technologies is difficult to use for direct comparison due to variation in modelling assumptions such as type of fuel used, scale of power output and efficiencies of individual process units. Furthermore, there is no study available to our knowledge, which provides a comparison between CLC and oxy-fuel combustion technologies for IGCC power plants. In this work, we compared IGCC–CLC, CDCLC, pre-combustion and oxy-fuel combustion technologies through simulation studies using common modelling assumptions and considerations. A detailed comparison with the conventional post-combustion technology was not included in this work. Interested readers are directed to publications such asKunze and Spliethoff [19] for a comparison between this and other technologies. The above four capture technologies were analysed against a conventional IGCC process without capture in order to estimate the energy penalty associated with CO_2 capture. An exergy analysis was also performed for IGCC–CLC, CDCLC and conventional IGCC processes to understand the fuel conversion mechanism and to find out the sources of irreversibilities in each process. Power production, power consumption, electrical efficiency, CO_2 capture efficiency and exergy are the key parameters studied in this work.

This work is solely based on the technical aspects of the CO_2 capture technologies. A comparison of cost of electricity for different capture technologies and commercial feasibility of carbon capture and storage will be considered in future publications. It should be also noted that the aim of this work is not to produce a plant design better than those proposed previously. Instead, the focus is on producing a consistent comparison between a numbers of technologies reported in the literature.

Methodology

Flowsheet models of five large-scale IGCC processes with and without CO_2 capture (see Table 1) were developed in Aspen plus in order to investigate the effect of CO_2 capture on net electrical efficiency and to allow comparisons of the capture technologies. The Aspen plus flowsheet models for the CO_2 capture cases (Cases 2–5) are provided in Supplementary information Fig. S1–S4. A nominal net power output between 400 and 500 MW was selected for all five cases. Table 2 shows the composition of Illinois #6 type coal used as fuel in all five cases. A conventional IGCC plant without CO_2 capture (Case 1) is considered as the base case. Cases 2 and 3 represent IGCC processes with pre- and oxy-fuel combustion based CO_2 capture, respectively. Case 4 is IGCC–CLC process and Case 5 is the CDCLC process with CO_2 capture. A block diagram of Cases 2–5 is shown in Figs. 1–4. Process configuration for Cases 2–5 is discussed in Section "Plant configuration". Individual unit models used in the processes for existing technology, such as water–gas shift reactor, gasifier, GT, steam turbine (ST), heat exchangers, are mostly verified by supplier data described in [22,23]. Development of Aspen plus flowsheet models for all five cases is explained in Section "Developing an industrial level flowsheet model in Aspen plus' while the methodology followed for exergy analysis is described in Section "Exergy analysis". Chemical and phase equilibrium based on Gibbs free energy minimisation is utilised

Table 1
Description of different cases used in our study.

Case no.	CO_2 capture technology used	CO_2 capture
1	Conventional IGCC	No
2	IGCC with physical absorption based pre-combustion capture	Yes
3	IGCC with oxy-fuel combustion	Yes
4	IGCC–CLC	Yes
5	CDCLC	Yes

Table 2
Composition of Illinois #6 coal [14,42].

Proximity analysis		
Items	Weight as received (%)	Dry weight (%)
Moisture	11.12	–
Fixed carbon	44.19	49.72
Volatiles	34.99	39.37
Ash	9.70	10.91
Total	100.00	100.00
HHV (MJ/kg)	27.13	30.53
Ultimate analysis		
Moisture	11.12	–
Ash	9.70	10.91
Carbon	63.75	71.72
H_2	4.5	5.06
N_2	1.25	1.41
Chlorine	0.29	0.33
Sulphur	2.51	2.82
O_2	6.88	7.75
Sulphate analysis		
Pyritic	–	1.70
Sulphate	–	0.02
Organic	–	1.10

Fig. 2. Simplified block diagram for IGCC with oxy-fuel combustion technology for CO_2 capture (Case 3).

to develop the reactor models in our simulations. Input parameters and design assumptions such as flow rates, pressure, temperature, equipment efficiency and fuel composition used for developing the process flowsheet models are collected from the various published literatures and are presented in Table 3. No external energy sources were used apart from the coal feed.

Plant configuration

IGCC with pre-combustion based CO_2 capture technology

This section describes the detailed plant configuration for IGCC with pre-combustion capture technology, Case 2 (see Fig. 1). A dry-feed entrained flow gasifier by Shell operating at 1300 °C and 30 atm is fed with crushed Illinoi #6 type coal (pressurised in a lock-hopper) and oxygen from the top [24]. A stand-alone ASU produces 95% pure oxygen (by volume) at 2.37 bar; the oxygen stream is compressed to 1.2 times the gasifier pressure before being fed into the gasifier [18,25]. The purge N_2 stream from the
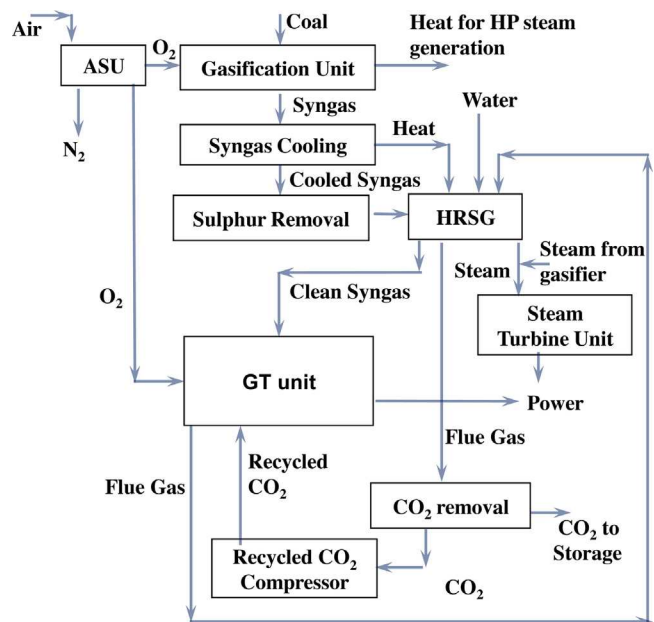
ASU is compressed to 22 atm and fed to the GT combustor for nitrogen oxides (NO_x) control. Inside the gasifier, the oxygen partially oxidises solid coal into syngas, which mainly consists of CO and H_2, with a conversion efficiency of 99.99% [11]. All reactions in the gasifier are assumed to achieve equilibrium. The ash present in coal feed melts at 1300 °C and exits the bottom of the gasifier, along with syngas [18].

The gasification of coal is highly exothermic and produces more heat than actually required to maintain the operating temperature of 1300 °C inside the gasifier. This excess heat is removed from the gasifier by passing pressurised water through cooling coils; water is ultimately converted to steam and used in the ultra-supercritical Rankine cycle for power generation [24]. Hot and pressurised raw syngas (at 1300 °C, 30 atm) from the gasifier is cooled to 350 °C in the heat recovery steam generation (HRSG) unit. This cooled raw
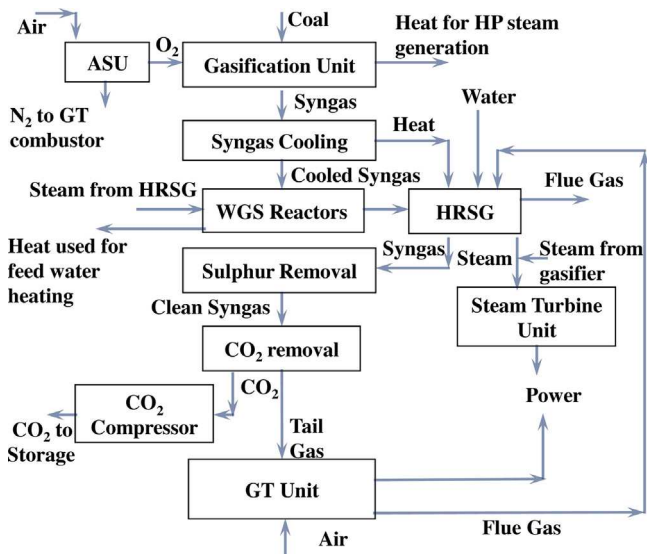

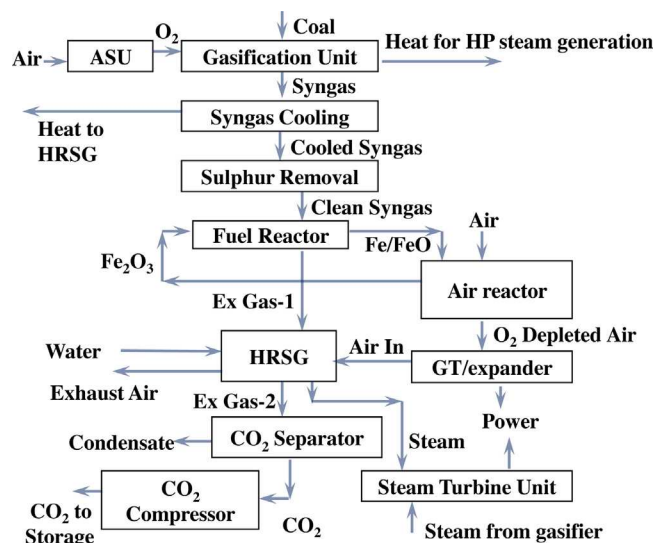**Fig. 1.** Simplified block diagram for IGCC with pre-combustion based CO_2 capture technology (Case 2).

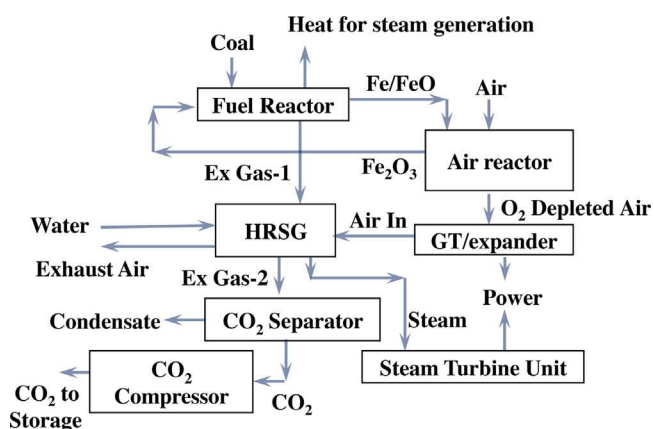**Fig. 3.** Simplified block diagram for IGCC–CLC process (Case 4).

Fig. 4. Simplified block diagram for CDCLC process (Case 5).

Unit	Parameters
Air Separation Unit	O_2 purity: 95% (vol.)
	ASU O_2 and N_2 delivery pressure: 2.37 atm
	Power consumption: 225 kWh/t O_2
	O_2 compression pressure: 36 atm
	N_2 compression pressure: 22 atm in Cases 1 and 2; 31 atm in Case 4
	O_2 and N_2 compressor efficiency: 83%
Gasifier reactor (entrained flow shell)	O_2/coal ratio (kg/kg): 0.867
	O_2 pressure to gasifier: 36 atm
	Gasification pressure: 30 atm
	Gasification temperature: 1300 °C (slagging conditions)
	Carbon conversion: 99.9%
	No pressure drop
	Gas cooling: Radiative and conductive heat exchanger
	Electric power for gasification aux: 1% of input fuel LHV
	HP steam raised in Gasification Island: 285 bar/600 °C
Acid Gas removal (AGR) unit for H_2S capture	Solvent: Selexol® (dimethyl ethers of polyethylene glycol)
	Overall H_2S removal yield: 99.5–99.9%
	Solvent regeneration: thermal (heat)
WGS unit	Two shift reactors WGS-1 and WGS-2 (equilibrium reactors)
	Temperature: 350 °C in WGS-1 and 178 °C in WGS-2
	Pressure: 30 atm in both WGS reactors
	CO conversion: 98%
	Steam/CO ratio: 2.11
Acid gas removal or CO_2 removal unit (Case 2)	Solvent: Selexol (dimethyl ethers of polyethylene glycol)
	Overall CO_2 removal yield in the AGR unit: 95–97%
	Solvent regeneration: pressure flash
Chemical looping combustion unit (Case 4)	Fuel reactor parameters: 30 atm/1100–1300 °C
	Air reactor parameters: 30 atm/1300 °C
	Gibbs free energy minimisation model for both reactors
	No pressure drop
CO_2 compression and drying	Delivery pressure: 150 atm
	Delivery temperature: 40 °C
	Compressor efficiency: 85%
GT/expander	Isentropic efficiency: 88%;
	GT/expander number: 1
	Discharge pressure: 1.05 atm;
	Pressure ratio: 21
	Turbine inlet temperature (TIT): 1300 °C
	Turbine outlet temperature (TOT): 500–550 °C
Steam turbines and HRSG	Three level pressures (HP/IP/LP): 285/36/6.5 bar
	Isentropic efficiency: 86%
	IP and LP reheat to 600 °C
	Condenser pressure: 0.046 bar
	Integration of steam generated in gasification island, syngas treatment, combined cycle GT/expander chemical looping unit
	$\Delta T_{min} = 10$ °C with no pressure drop

syngas along with pressurised steam (350 °C; 30 atm) generated in the HRSG is fed to a water–gas shift reactor (WGS-1) operating at 350 °C and 30 atm, where CO is partially converted to CO_2 by reaction with steam. The exhaust gases from WGS-1 containing partially converted syngas and steam is cooled to 178 °C in the HRSG and fed to reactor WGS-2 which operates at 178 °C and 30 atm, for further conversion of CO into CO_2 [26]. The cumulative CO conversion efficiency for both the WGS reactors is 98% [27,28]. The shift reactions inside the two WGS reactors are exothermic in nature (44.5 kJ/mol), therefore any excess heat generated is extracted by pressurised feed water in order to maintain the operating temperature conditions inside the reactors [18].

The exhaust gaseous stream from WGS-2 reactor is principally composed of a mixture of CO_2, CO, H_2 and steam, which is cooled to 40 °C in the HRSG before being fed into the acid gas removal (AGR) unit; where 99.99% hydrogen sulphide (H_2S) and 94.8% CO_2 is removed. The AGR unit uses a Selexol-based physical solvent, which is regenerated in a steam stripper in the H_2S removal unit and pressure flash chambers in the CO_2 removal unit [28,29]. Steam required in the steam stripper is generated in the HRSG at 130 °C. CO_2 recovered from Selexol solvent is compressed to 150 atm for transportation and storage. Clean syngas after H_2S and CO_2 removal is heated in the HRSG to 300 °C and fed to the GT combustor (maintained at 1300 °C and 21 atm) for combustion in the presence of compressed atmospheric air. Excess air supply along with N_2 from the ASU maintains the required temperature of 1300 °C inside the GT combustor. Flue gas leaving the GT at 597 °C is sent to the HRSG for heat recovery before venting to the atmosphere.

In the Rankine cycle, pressurised steam is generated at 600 °C through a two-step process [18]. In step one, only supercritical steam is produced at 600 °C and 285 bar by using the excess heat generated in the reactor units; WGS reactors and gasifier in Case 2. In step two, heat available from the cooling of process streams (raw syngas from gasifier, exhaust from the two WGS reactors and GT in Case 2) in the HRSG is used for (i) generating supercritical (285 bar) steam at 600 °C, and (ii) reheating intermediate pressure (IP) and low pressure (LP) steam to 600 °C. The supercritical steam produced in both steps is mixed and supplied to the HP steam turbine (ST). The exhaust steam from the LP ST exits at 0.046 bar and 90.5 °C [11] . It is then condensed at 25 °C using cooling water at 15 °C and pumped back to the relevant process units after pressurising to 285 bar. The steam generation approach followed is similar for all five cases.

IGCC with oxy-fuel combustion technology for CO_2 capture

In IGCC with oxy-fuel combustion technology (see Fig. 2), the coal gasification process is same as in Case 2 described in

Section "IGCC with pre-combustion based CO_2 capture technology". Downstream of the gasifier, raw syngas (at 1300 °C; 30 atm) is cooled to 40 °C in the HRSG and sent to the Selexol-based AGR unit for sulphur removal. The clean syngas after H_2S removal is re-heated to 300 °C in the HRSG before being fed to the GT combustor operated at 1300 °C and 21 atm. A stream of pure oxygen generated in the ASU is compressed and supplied to the GT combustor (instead of atmospheric air) for complete syngas conversion [19]. This arrangement prevents dilution of flue gas with N_2. The GT exhaust consisting primarily of CO_2 and water vapour is sent for heat recovery in the HRSG, where the vapour is condensed and

Table 4
Water and steam cycle details for IGCC–CLC process (Case 4).

Stream	Flow rate (t/h)	Inlet temperature (°C)	Outlet temperature (°C)	Pressure (bar)
HP steam produced in gasifier,	111.6	25.0	600.0	285.0
HP steam from HRSG	395.5	25.0	600.0	285.0
HP steam to HP ST	507.1	600.0	277.3	285.0
IP steam to IP reheater	507.1	382.2	600.0	36.0
IP steam to IP ST	507.1	600.0	361.2	36.0
LP steam to LP reheater	507.1	384.0	600.0	6.5
LP steam to LP ST	507.1	600.0	90.6	6.5
Cooling water to steam condenser	43,200.0	15.0	25.5	2.0
Condensate return to HRSG	395.5	25.0	600.0	285.0

separated from CO_2. Nearly 80% (by mass) of this CO_2 stream is compressed and recycled to the GT combustor to maintain the operating temperature of 1300 °C [20]. The remaining 20% of CO_2 is compressed to 150 atm for storage. In the Rankine cycle, pressurised steam is produced using a two-step process (as in Case 2). In step one, supercritical steam at 600 °C and 285 bar is produced using the excess heat generated in the gasifier. In step two, heat available from cooling of raw syngas and GT exhaust in HRSG is used for supercritical steam generation and for reheating IP and LP steam to 600 °C. Steam produced in both the steps is mixed and supplied to the three (HP, IP and LP) STs.

IGCC–CLC process for CO_2 capture

The IGCC–CLC process (Case 4; see Fig. 3) follows the same process configuration as in Case 3, which is discussed in Section "IGCC with oxy-fuel combustion technology for CO_2 capture", until the sulphur removal unit. The sulphur free syngas is heated to 300 °C in the HRSG and sent to the counter-current fluidised bed fuel reactor (operating at 1280–1300 °C and 30 atm), where it is completely oxidised following reactions shown in Eqs. (1) and (2). The oxygen required for syngas conversion is supplied by the OC particles (hematite) which are reduced to wustite ($Fe_{0.947}O$). Fe_2O_3 is supported by 15% aluminium oxide (Al_2O_3) and 15% silicon carbide (SiC) to enhance its thermal and physical properties [30]. A syngas conversion efficiency of ~100% is achieved in the fuel reactor [10,11,31]. The exhaust from the fuel reactor is passed through a cyclone separator where the reduced OC particles are separated from gaseous products of syngas conversion primarily consisting of CO_2 and vapour. This hot gaseous product stream is cooled in the HRSG to condense the vapour and produce a pure CO_2 stream for compression and storage.

Reduced OC particles ($Fe_{0.947}O$) are fed to CLC air reactor where they are fully re-oxidised to Fe_2O_3 by pressurised air, which also helps in circulation of OC in the system. The OC regeneration process shown in Eq. (3) is highly exothermic, therefore excess air along with N_2 from ASU is supplied to the air reactor to maintain the operating temperature of 1300 °C [12]. Regenerated OC (Fe_2O_3) and oxygen depleted air exits the air reactor at 1300 °C and 30 atm and are separated in the cyclone. The gases are passed through an expander (also referred as Gt in this work) followed by the HRSG before finally venting them to atmosphere. OC particles recovered in cyclone are recycled to the fuel reactor. The CLC reactor models are validated with experimental results available in literature [32–34]. Steam generation/reheat for Case 4 follows the same approach as discussed in Case 3. Table 4 presents the water and steam cycle details for Case 4.

$$CO + Fe_2O_3 \rightarrow CO_2 + 2Fe_{0.947}O \tag{1}$$

$$H_2 + Fe_2O_3 \rightarrow H_2O + 2Fe_{0.947}O \tag{2}$$

$$2Fe_{0.947}O + \frac{1}{2}O_2 \rightarrow Fe_2O_3 \tag{3}$$

Supplementary information Table S2 and Fig. S5 show the details on the composition and thermodynamic state of key process streams and the heat transfer diagram, respectively, for Case 4 as an example case.

CDCLC process for CO_2 capture

In the CDCLC process (Case 5; see Fig. 4), the pulverised coal is directly fed to the fuel reactor, eliminating use of any separate gasifier. Coal is oxidised by the OC in the fuel reactor. Almost complete coal conversion is calculated by the equilibrium based fuel reactor model. The simulation results were validated via comparison with available literature on experimental data and modelling [32,35–42]. Exhaust product gas from the fuel reactor consisting primarily of CO_2 and water vapour is separated from the reduced OC particles in a cyclone. Reduced OCs are sent to the air reactor for regeneration, whereas hot product gas is cooled to 40 °C in the HRSG and sent to gas clean-up and the AGR unit for sulphur removal. Steam required for Selexol regeneration is generated in the HRSG. Any remaining vapour is condensed, yielding a stream of pure CO_2 for compression and storage. A 100% CO_2 capture rate was observed [16]. Regenerated OC from the air reactor follows the same path as in Case 4 (IGCC–CLC) described in Section "IGCC–CLC process for CO_2 capture". The supercritical steam at 600 °C and 285 bar is generated in the HRSG by using a portion of heat available from the product gas (from the fuel reactor) and flue gas (from the GT) cooling. The IP and LP steam are heated to 600 °C in the HRSG.

Developing an industrial level flowsheet model in Aspen plus

Tables 2 and 3 present the key parameters and operating conditions used in development of the flowsheet models for the cases mentioned in Section "Plant configuration". Stream class MIXCINC is selected for all the cases considered in this study. The Peng–Robinson–Boston–Mathias (PR-BM) property method is used for the conventional components whereas coal enthalpy models HCOALGEN and DCOALIGT are used for the two non-conventional components coal and ash [43,44]. OC is entered as solid particle in the component list. The equilibrium reactor model RGIBBS is used for modelling the coal gasifier, fuel reactor, air reactor and combustor. The RGIBBS model requires temperature, pressure, stream flow rate and composition as its key inputs. The REQUIL model is used to design the two WGS reactors. A PUMP model with an efficiency of 90% is used to pressurise the feed water in the process. A counter-current MHeatX type heat exchanger is used to represent the HRSG. An MCOMPR model with an isentropic efficiency of 83% represents the four-stage compressor used in the processes to compress the gas streams such as air, oxygen, N_2 and CO_2.

Table 5
Plant performance indicators for IGCC–CLC, pre-combustion and oxy-fuel combustion processes obtained by Aspen plus simulations.

Plant data	Units	Conv. IGCC Case 1	Pre-combustion Case 2	Oxy-fuel combustion Case 3	IGCC–CLC Case 4
Fuel input energy, LHV (A)	MWth	1126.50	1126.50	1126.50	1126.50
Net GT output	MWe	335.84	293.12	256.53	259.85
ST output	MWe	239.99	230.19	277.94	281.08
Gross electric power output (B)	MWe	575.83	523.31	534.47	540.93
ASU consumption + O_2 compression	MWe	34.10	34.10	86.84	34.10
CO_2 capture and compression	MWe	0.00	27.60	34.47	10.20
Power cycle pumps	MWe	5.39	5.38	6.09	6.64
Other	MWe	37.80	37.80	11.26	42.27
Total parasitic power consumption (C)	MWe	77.28	104.88	138.66	93.21
Net electric power output (D = B − C)	MWe	498.54	418.43	395.80	447.72
Gross electrical efficiency (B/A × 100)	%	51.12	46.45	47.44	48.02
Net electrical efficiency (D/A × 100)	%	44.26	37.14	35.15	39.74
CO_2 capture efficiency	%	0.00	94.80	∼100	∼100
CO_2 emission	t/h	328.30	17.00	0.30	0.60
CO_2 specific emissions	t/MWh	0.659	0.041	0.001	0.001
CO_2 captured	t/h	0.00	313.00	328.30	328.30
Electric output per ton of CO_2 captured	MWh/t	–	1.34	1.21	1.36

Exergy analysis

The energy analysis based on the first law of thermodynamics does not offer sufficient information on the potential work lost in transforming energy in various processes [45]. The irreversibility in a process can be accounted for by a detailed exergy analysis, which uses the first and second law of thermodynamics together. Kotas [45] defined the exergy of a stream is the maximum amount of work obtainable when the stream is brought from its initial state to the dead state by processes during which the stream may interact only with the environment. The dead state or reference state considered in this study for exergy calculation is 25 °C (T_0) and 1 atm (P_0). The exergy of a process stream can be divided into two parts: physical exergy and chemical exergy as shown in Eq. (4) [46].

$$Ex_{total} = Ex_{ph} + Ex_{ch} \tag{4}$$

The physical exergy (Ex_{ph}) is the maximum useful work obtained by passing the unit of mass of a substance of the generic state (T, P) to the environmental/reference state (T_0, P_0) through purely physical processes [47–49]. The physical exergy component is then given by Eq. (5).

$$Ex_{ph} = (H - H_0) - T_0(S - S_0) \tag{5}$$

where H and S are specific molar enthalpy (kJ/kmol) and specific molar entropy (kJ/kmol K), respectively; H_0 and S_0 are the values of H and S at standard conditions (T_0, P_0). Chemical exergy is the maximum useful energy, which would be attained by passing from the environmental state to the dead state, by means of chemical processes with reactants and products at the environmental temperature and pressure, when the stream composition is not in chemical equilibrium with the environment [48,50]. The chemical exergy of a stream is expressed in Eq. (6).

$$Ex_{ch_{total}} = \sum_i x_i Ex_{ch_i} + RT_0 \sum_i x_i \ln x_i \tag{6}$$

where x_i and Ex_{ch_i} are molar fraction and molar chemical exergy (kJ/kmol), respectively, of each component in the mixture, and R is the universal gas constant. Exergy destruction (Ex_d) of each individual unit can be calculated by finding the difference between the exergy of input and output streams of this unit as shown in Eq. (7) [51]. The exergetic efficiency of each individual unit is calculated by Eq. (8) [52]. The overall exergetic efficiency of the process considered in our study is the ratio of net power produced in the process to the total exergy input (the total chemical exergy of

the coal), shown in Eq. (9) [53].

$$Ex_d = \sum Ex_{in} - \sum Ex_{out} \tag{7}$$

$$Ex_{eff,unit} = \frac{\sum Ex_{out}}{\sum Ex_{in}} \tag{8}$$

$$Ex_{eff,overall} = \frac{\text{Net power output}}{\text{Chemical exergy of coal input}} \tag{9}$$

The chemical exergy of coal is calculated using Eq. (10) [52,54]. The terms CV, w, h_{fg} and s in Eq. (10) represents the net calorific value of coal in kJ/kg, percentage of moisture content in coal, latent heat of water in kJ/kg at temperature T_0 and mass fraction of sulphur in the coal, respectively. The value of φ_{dry} is estimated from the Eq. (11). The terms h, c, o and n denote the mass fraction of H_2, carbon, oxygen and N_2, respectively, in coal.

$$Ex_{ch,coal} = (CV + w \times h_{fg})\varphi dry + 9417s \tag{10}$$

$$\varphi_{dry} = 0.1882\frac{h}{c} + 0.061\frac{o}{c} + 0.0404\frac{n}{c} + 1.0437 \tag{11}$$

Results and discussion

IGCC–CLC process against conventional IGCC process

The performance of the IGCC–CLC process (Case 4) and conventional IGCC process (Case 1) are compared on the basis of net electrical efficiency and CO_2 emissions. Detailed simulation results for both cases are summarised in Table 5. Case 1 is not equipped with CO_2 capture and emits 328.3 t/h of CO_2. In contrast, Case 4 with CO_2 capture emits only 0.60 t/h of CO_2 capturing 99.8% CO_2 emissions. This syngas conversion efficiency obtained by the equilibrium reactor models (RGIBBS reactor model in Aspen plus) for CLC fuel reactor in our simulation is similar to the efficiency given in Jerndal et al. [74] and Chiu and Ku [31]. Case 4 gives an overall electrical efficiency of 39.69%, which is somewhat higher than is observed in other work [10,12,55]. This could be due to the use of a supercritical steam cycle (hence, a higher top pressure and temperature in the steam cycle and consequently higher overall efficiency, see [56]) in our case whereas the other studies used sub-
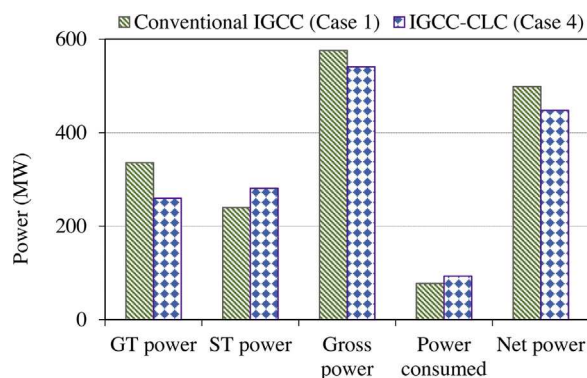
Fig. 5. Relation between GT, ST, gross, consumed and net power output for Cases 1 and 4.

critical steam. CO_2 capture in Case 4 contributes to a net electrical efficiency penalty of 4.57%-points compared to Case 1, which has 44.26% efficiency. Results obtained for the efficiency of Cases 1 and 4 can be compared to various other studies including IEA reports [1,3,57,58]. The above comparison concludes that almost 100% CO_2 can be captured from an IGCC power plant (using CLC) with ∼10% reduction in the net electricity produced per unit of fuel input.

Fig. 5 shows the relations between power produced and consumed in different units for Cases 1 and 4. The overall heat produced (Q_{total}) from syngas conversion in both the cases is same. In Case 1, this overall heat is completely produced in a single combustor reactor, the exhaust gases of which are first used in the GT unit for power generation and then in the HRSG for heat recovery. In contrast to Case 1, Case 4 combusts the syngas in two separate reactors; the air and fuel reactors, ($Q_{total} = Q_{air\ reactor} + Q_{fuel\ reactor}$). The GT in Case 4 receives less energy input ($Q_{air\ reactor}$) for power production since it is supplied with the exhaust gases from the air reactor only (i.e. $Q_{air\ reactor}$) and hence it produces 76 MW lower power than the GT in Case 1. The heat generated in the fuel reactor ($Q_{fuel\ reactor}$) in Case 4 is used in Rankine cycle which results in 41.2 MW more power output in STs compared to Case 1. Case 1 generates 51 MW higher net power than Case 4 because in Case 1 most of the heat available from syngas conversion is used in the GT cycle which is more efficient than the Rankine cycle to convert heat into power. In addition, the parasitic energy consumption in Case 4 is 20% higher than in Case 1, which is mainly because of the extra energy required for CO_2 removal and compression.

Comparison of CLC with pre-combustion and oxy-fuel combustion technologies

The competitiveness of CLC with pre-combustion and oxy-fuel combustion technologies is investigated here on the basis of CO_2 capture and net electrical efficiency. The calculated process outputs summarised in Table 5 indicate that Case 4 with the IGCC–CLC process has the highest net electrical efficiency of 39.74%. The next highest is 37.14% for IGCC with physical absorption based pre-combustion capture technology (Case 2) followed by 35.15% for the IGCC with oxy-fuel combustion process (Case 3). The efficiency penalty associated with CO_2 capture in Cases 2, 3 and 4 compared to the conventional IGCC process without capture (Case 1) ranges between 5 and 9%-points, which is comparable to other literature values [10,29,59–61]. The net electrical efficiencies achieved by the above three capture technologies are found to be substantially higher than those for amine based post-combustion capture technology [62].

Cases 3 and 4 capture ∼100% CO_2 compared to 94.8% for Case 2. The CO_2 capture efficiencies for Cases 2–4 are comparable to various other studies [10,11,20,58,62]. The lower capture efficiency
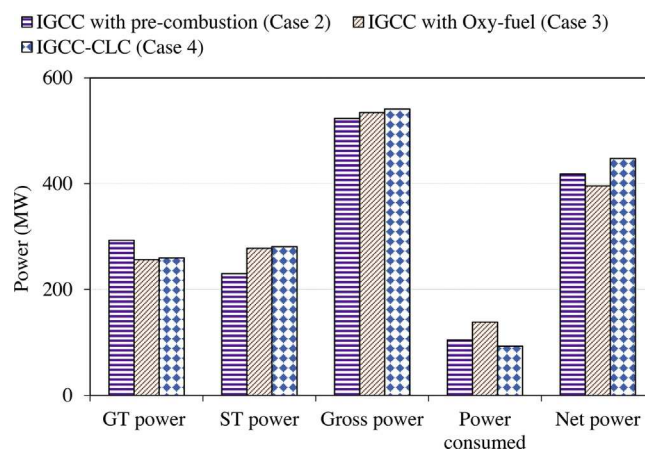

Fig. 6. Relation between GT, ST, gross, consumed and net power output for Cases 2–4.

in Case 2 is due to (i) incomplete absorption of CO_2 (∼95–97%) by the Selexol solvent, and (ii) 98% CO conversion in the two WGS reactors. The unconverted CO from the WGS-2 reactor is not captured by the Selexol solvent in the AGR unit and is converted into CO_2 in the GT combustor. This CO_2 along with the un-captured CO_2 from the AGR unit is expanded in the GT before it is finally vented to the atmosphere with other flue gases.

Fig. 6 shows the variation in power production and power consumption in Cases 2–4. Case 2 produces 293.12 MW power from GT which is higher by 36.6 and 33.27 MW than Cases 3 and 4, respectively. In spite of producing the highest GT power, Case 2 manages to generate only 523.31 MW of gross power (lowest among Cases 2–4), owing to the lowest power output (230.19 MW) in the Rankine cycle or the STs compared to Case 3 (277.94 MW) and 4 (281.08 MW). However, the net power output is lowest for Case 3 (395.80 MW) and not Case 2 (418.43 MW) since the parasitic energy consumption in Case 3 is 32.2% more than Case 2 due to the high oxygen demand and compression effort for recycling CO_2 into the GT combustor to assist in temperature moderation. On the other hand, Case 4 with the highest gross power of 540.93 MW and lowest parasitic power of 93.21 MW along with ∼100% CO_2 capture proves to be superior in all aspects.

Table 6 shows the energy and efficiency penalty associated with CO_2 capture in Cases 2–4 with reference to the conventional IGCC process without capture (Case 1). Table 6 indicates that the relative decrease in net electrical efficiency in Case 2, 3 and 4 against Case 1 is 16.08, 20.58 and 10.21%, respectively. These values are lower compared to the amine based post-combustion capture methods described in a report of the IEA [62], which indicates that IGCC with pre-combustion, oxy-fuel combustion or CLC technologies is likely more efficient than the PC power plants with post-combustion capture technology for CO_2 capture. Per MW decrease in the net energy production with reference to Case 1, the IGCC–CLC process captures significantly higher (6.46 t/h) CO_2 compared to pre-combustion (4.10 t/h) and oxy-fuel combustion (3.04 t/h) capture technologies. These results suggest that CLC is a more favourable option from energetic point of view (without economic considerations) to capture CO_2 from IGCC power plants compared to pre-combustion and oxy-fuel combustion technologies. However, pre-combustion and oxy-fuel combustion are practically proven and commercially available technologies whereas CLC requires a considerable amount of further research to make it available for commercial use [7,18,62,63].

Hanak et al. [69], Xu et al. [73] and IEA [70] reported a loss of ∼10% points, 11–16% points and 10–12% points in the net electrical efficiency, respectively, for a supercritical coal-fired power plant

Table 6
CO$_2$ captured per unit energy and efficiency penalty with reference to conventional IGCC process (Case 1).

Plant data	Units	IGCC–CLC Case 4	Pre-combustion Case 2	Oxy-fuel combustion Case 3
Energy penalty (A)	MW	50.82	80.11	102.74
CO$_2$ captured (B)	t/h	328.30	328.30	313.00
CO$_2$ captured per MW decrease in energy production than Case1 (C = B/A)	t	6.46	4.10	3.04
Net electrical efficiency (D)	%	39.74	37.14	35.15
Net electrical efficiency penalty compared to Case 1 (E = 44.26−D)	%	4.52	7.12	9.11
Relative decrease in net electrical efficiency compared to Case 1 (F = E × 100/44.26)	%	10.21	16.08	20.58
CO$_2$ captured per unit decrease in net electrical efficiency from Case 1 (B/E)	t	72.63	46.11	34.35

using monoethanolamine (MEA) based post-combustion CO$_2$ capture technology, which is higher compared to our IGCC-CLC process (Case 4) showing a loss of 4.52% points. Furthermore, a 14.5–15.0% loss in the net electrical efficiency was observed by Sanpasertparnich et al. [72] and Kanniche et al. [59] for pulverised coal power plants using amine based post-combustion CO$_2$ capture technology. It is also noted in the above mentioned studies that the amine based post-combustion capture technologies captured up to 90% CO$_2$ which is lower by ∼10% points compared to the IGCC–CLC process studied in our work. Based on the above comparisons it can be concluded that IGCC–CLC process is more efficient that amine based post combustion process from the energetic point of view.

Comparison of CDCLC process with all other cases

One of the main objectives of this work is to indicate the potential improvements or changes that could be made to the process configuration for CLC technology in order to make it more energy efficient, and simultaneously compare it with the conventional IGCC process without CO$_2$ capture (Case 1) and other CO$_2$ capture technologies. In order to achieve the above objective, the IGCC–CLC process (Case 4) was modified to CDCLC process (Case 5) which uses coal directly in the CLC fuel reactor instead of syngas and hence, completely eliminates the use of the additional coal gasifier which was used in all other cases (see Section "CDCLC process for CO$_2$ capture" for details).

Table 7 shows the key performance characteristics of the CDCLC process along with the results of its comparison to Cases 1–4. No significant difference was observed in the net electrical efficiencies of the CDCLC process (44.42%) and conventional IGCC process (44.26%). A similar trend has been witnessed for exergetic efficiency by Anheden and Svedberg [64] with syngas used as fuel instead of coal. They found that CLC causes lower destruction of fuel exergy upon combustion compared to conventional combustion process, which could result in higher net power generation in CLC process. A more detailed discussion on the power output trend of the CDCLC process in comparison to the conventional IGCC process is presented in Section "Exergy analysis of conventional IGCC, IGCC–CLC and CDCLC processes" through

exergy analysis. The net electrical efficiency obtained for the CDCLC process in our work is higher than that observed in other available literatures [10,13,14]. As mentioned previously, this is likely owing to the assumed (potentially optimistic) steam cycle conditions simulated here.

The CDCLC process shows an increase of 4.67%-points in the net electrical efficiency compared with IGCC–CLC process (Case 4), which indicates an improvement in the overall performance of the CLC technology while maintaining ∼100% CO$_2$ capture rate. The coal conversion efficiency obtained in the fuel reactor in our simulation is similar to the efficiency obtained by Fan et al. [13]. The gross power output of the CDCLC process is 526.33 MW, which is lower than Cases 1, 3 and 4; however, it still manages to produce 1.8–82 MW higher net electrical power. This is because the CDCLC process has very small parasitic power consumption (i.e. the usage of electricity by auxiliary equipment such as compressors and pumps) of 25.98 MW, primarily due to the absence of an ASU and a N$_2$ compressor. IGCC with oxy-fuel combustion technology (Case 3) has the highest relative decrease (20.90%) in net electrical efficiency with respect to CDCLC process. To summarise, using coal directly in the CLC fuel reactor instead of syngas can significantly reduce the energy penalty associated with CO$_2$ capture and produce a similar amount of net electricity as that produced by a conventional IGCC process without CO$_2$ capture. It can be concluded from the above discussion that CDCLC is more energy efficient than IGCC–CLC. However, the solid–solid reactions between coal and OC in the fuel reactor (even if mediated by gas phase species such as CO/CO$_2$) of the CDCLC process are comparatively more complicated and slower than the gas–solid reactions in the fuel reactor of IGCC–CLC process which provides an advantage to IGCC–CLC process over CDCLC.

Exergy analysis of conventional IGCC, IGCC–CLC and CDCLC processes

An exergy analysis has been conducted to identify the sources of irreversibilities in the conventional IGCC (Case 1), IGCC–CLC (Case 4) and CDCLC (Case 5) plant designs. Exergy destruction within each process unit can be estimated using an exergy balance equation (see Section "Exergy analysis"). A visual basic application

Table 7
Comparison of plant data for CDCLC process with conventional IGCC, pre-combustion, oxy-fuel combustion and IGCC–CLC processes.

Plant data	Units	CDCLC Case 5, A	Differences [(B/C/D/E) − A]			
			Conv. IGCC Case 1, B	Pre-combustion Case 2, C	Oxy-fuel combustion Case 3, D	IGCC–CLC Case 4, E
GT output	MWe	289.78	46.06	3.34	−33.25	−29.93
St output	MWe	236.55	3.44	−6.36	41.39	44.53
Gross power output	MWe	526.33	49.50	−3.02	8.14	14.60
Power consumed	MWe	25.98	51.30	78.89	112.68	67.22
Net power output	MWe	500.35	−1.81	−81.92	−104.55	−52.63
Net electrical efficiency	%	44.42	−0.16	−7.27	−9.27	−4.67
Relative decrease in net electrical efficiency in reference to Case 1	%	0	–	16.08	20.58	10.21

Note: negative sign indicate that the CDCLC process has higher values for the corresponding plant data.

for Microsoft® Excel 2013 developed by Querol et al. [71] has been used to calculate the exergies of individual streams in the Aspen plus simulation models. It is worth noting that the actual exergy values could be marginally different than the exergy values calculated in the current work. This is because only physical and chemical exergies of the streams were considered whereas the exergy of mixing is excluded from the total exergy calculations. The authors consider that since this work is a comparative study (and also the exergy of mixing is comparatively very small), the exclusion of exergy of mixing from total exergy calculations does not have any significant impact on the results or conclusions of the current work. The total exergy lost in the overall process is a combination of the exergy contained in the material streams discharged from the overall process without further usage and the exergy destruction in various process units such as the gasifier, CLC reactors, combustor, turbines, compressors and pumps. We considered the recovered sulphur stream as an exergy loss in our analysis, although sulphur is a useful by product and can be sold under some circumstances. Table 8 lists the exergy destruction rates in the main process blocks and the energetic efficiency of the overall process for Cases 1, 4 and 5.

The exergy analysis results indicate that the fuel reactor of IGCC-CLC process can oxidise syngas more efficiently with an exergy destruction rate of only 4%, compared to the combustor of a conventional IGCC process which experiences an exergy destruction rate of 17.5% for oxidising the same amount of syngas. Anheden and Svedberg [64] obtained an exergy destruction rate of 2.6–4.2% in the CLC fuel reactor and 22.9% in the IGCC combustor, which is comparable to our observations. In the IGCC–CLC process, the overall syngas conversion is a combination of the oxidation and reduction reactions taking place in the CLC fuel and air reactors. Therefore, the consideration of only the fuel reactor does not provide a fair comparison of the syngas conversion capabilities of IGCC–CLC and conventional IGCC processes, and it is essential to include the exergy destruction or losses of the CLC air reactor as well. The addition of the air reactor in the syngas conversion analysis increases the overall exergy destruction to 17.4% (in the combination of the fuel and air reactors), which is similar to what is obtained for the combustor unit. This implies that both IGCC–CLC and conventional IGCC are equally efficient in syngas conversion. The ASU, oxygen compressor and gasifier have a combined exergy destruction rate of 26.15% and are common to both IGCC–CLC and conventional IGCC processes. The gasifier in both IGCC–CLC and conventional IGCC processes, with an exergy destruction rate of 24.4%, is the most exergetically inefficient unit among all other process units.

The above discussion indicates that both IGCC–CLC and conventional IGCC processes are equally efficient in coal gasification and syngas conversion. Compared to the conventional IGCC process, a higher N_2 compression pressure in the IGCC–CLC process results in a rate of exergy destruction 0.12%-points higher. The exergy destruction rate in the GT and air compressor of IGCC–CLC process is 0.87%-points higher than conventional IGCC process. This is due to the increased airflow in the CLC air reactor caused by higher enthalpy of oxidation for the OCs than the conventional syngas combustion. The larger volumetric flow of water and steam through the pumps, HRSG and STs results in 1.16%-points higher exergy destruction in the Rankine cycle of the IGCC–CLC process compared to the conventional IGCC process. The extra CO_2 compressor used in the IGCC–CLC process (not used in conventional IGCC) creates 0.35%-points additional exergy destruction in compressing the captured CO_2 to 150 atm. Table 8 shows that the total exergy losses (exergy destruction + exergy lost in exhaust streams) in the IGCC–CLC process is 51.5 MW higher than for the conventional IGCC process. The above discussed points collectively explain the reason for lower overall exergetic efficiency of 35.6% in the IGCC–CLC process, compared to 39.7% in the conventional IGCC process. The exergy destruction rates and overall exergetic efficiency obtained for the IGCC–CLC and conventional IGCC processes in our study are comparable to other literatures [12,64].

The CDCLC process (Case 5) has an overall exergetic efficiency of 39.8%, which is 4.2%-points higher than the IGCC–CLC process and similar to the conventional IGCC process. The CDCLC process has the lowest exergy destruction of 756.1 MW as compared to 757.3 MW for conventional IGCC and 808.8 MW for IGCC–CLC process. It is seen from Table 8 that in CDCLC process, coal is more efficiently oxidised in the fuel reactor with an exergy destruction rate of 40.8% compared to 41.9% destruction in conventional IGCC process (exergy destruction in gasifier + combustor) and 41.8% destruction in the IGCC–CLC process (exergy destruction in gasifier + CLC fuel reactor). The absence of ASU, oxygen compressor and N_2 compressor benefits the CDCLC process by saving the additional exergy destruction associated with these units. The exergy destruction in the Rankine cycle of the CDCLC process is 2.57%-points and 3.73%-points lower than conventional IGCC and IGCC–CLC processes. This could be due to the lower mass flow of water/steam in the Rankine cycle and lesser number of streams available for heat transfer in the HRSG which reduces the number of heat exchangers and thus minimises the chances of exergy losses. The above discussed points explain the higher exergetic efficiency of CDCLC process than IGCC–CLC process. It is concluded that gasifying coal directly in the CLC fuel reactor ultimately reduces the total exergy losses (exergy destruction + exergy of exhaust streams) in the process by 6.5% (relative) and makes CLC technology equally efficient as the conventional IGCC process in terms of exergy.

Table 8
Exergy destruction rate and exergy loss for the conventional IGCC, IGCC–CLC and CDCLC systems.

	Units	Conv. IGCC Case 1	IGCC–CLC Case 4	CDCLC Case 5
Exergy destruction in gasifier	(%)	24.4	24.4	–
Exergy destruction in combustor	(%)	17.5	–	–
Exergy destruction in CLC reactor system	(%)	–	17.4	40.8
Total exergy destruction in fuel conversion	(%)	41.9	41.8	40.8
Exergy destruction in ASU and O_2 compressor	(%)	1.75	1.75	–
Exergy destruction in GT and air compressor	(%)	4.49	5.36	8.5
Exergy destruction in N_2 compressor	(%)	0.54	0.66	–
Exergy destruction in CO_2 compressor	(%)	–	0.35	0.35
Exergy destruction in sulphur removal and Rankine cycle	(%)	7.82	8.98	5.25
Total exergy destruction	(%)	56.5	58.9	54.9
Total exergy loss (exergy destruction + exergy of exhaust streams)	(%)	60.3	64.4	60.2
Total exergy loss (exergy destruction + exergy of exhaust streams)	(MW)	757.3	808.8	756.1
Net power produced	(MW)	498.54	447.72	500.35
Total exergetic efficiency of the process	(%)	39.7	35.6	39.8

Summary and conclusion

This article evaluates (via modelling in Aspen plus) the competitiveness of CLC technology against pre-combustion and oxy-fuel combustion technology for IGCC plants with CO_2 capture producing electricity from coal, in five different process configurations (four with, and one base-case without, CO_2 capture technology). Chemical Looping Combustion (CLC) was studied for two different process configurations, IGCC–CLC and CDCLC, in order to fully explore its potential. The work also examines the CLC technology through a detailed exergy analysis. The key conclusions obtained from this work are as follows:

- For IGCC cases with CO_2 capture (Cases 2–4), the IGCC–CLC process achieves the highest net electrical efficiency of 39.74% (capture efficiency ∼100%) followed by pre-combustion capture at 37.14% (capture efficiency ∼94.8%) and oxy-fuel combustion capture at 35.15% (capture efficiency ∼100%). These figures are relative to a net electrical efficiency of 44.26 for the unabated plant.
- Modification of the IGCC–CLC process to the CDCLC process (i.e. using the coal directly in the gasification process, rather than utilising a separate gasifier) increases the net electrical efficiency by 4.67%-points, while maintaining the CO_2 capture rate at 100%. The net electrical efficiency is then approximately equivalent to the base case unabated system (case 1).

The detailed comparative analysis performed in this work demonstrates that, regardless of any configuration used, the CLC technology is a more suitable option for CO_2 capture than physical absorption based pre-combustion capture and oxy-fuel combustion capture technologies from the thermodynamic perspective. However, it is necessary to examine the economic aspects (which is out of the scope of this work), before drawing firm conclusions regarding the selection of a capture technology. Furthermore, the impact of degradation of the OC for CLC and Selexol for physical absorption technologies should be examined for complete technoeconomic evaluation; life cycle analysis is also necessary for a complete understanding of the environmental impact of the process.

Competing interests

The authors declare no competing financial interest.

Acknowledgement

Appendix A. Supplementary data

Supplementary data associated with this article can be found, in the online version, at 10.1016/j.jece.2015.07.018.

References

[1] IEA, CO_2 Emissions from Fuel Combustion, International Energy Agency, 2012.
[2] BP, BP Statistical Review of World Energy, BP plc, 2014.
[3] IEA, World Energy Outlook, International Energy Agency, 2009.
[4] IEA, key World Energy Statistics, Key World Energy Statistics, International Energy Agency, 2013.
[5] WCI, Coal Meeting the Climate Challenge, World Coal Institute, 2009.
[6] S. Anderson, R. Newell, Prospects for carbon capture and storage technologies, Annu. Rev. Environ. Resour. 29 (1) (2004) 109–142, doi:http://dx.doi.org/10.1146/annurev.energy.29.082703.145619.
[7] M.E. Boot-Handford, J.C. Abanades, E.J. Anthony, M.J. Blunt, S. Brandani, N. Mac Dowell, J.R. Fernández, M. Ferrari, R. Gross, J.P. Hallett, R.S. Haszeldine, P. Heptonstall, A. Lyngfelt, Z. Makuch, E. Mangano, R.T.J. Porter, M. Pourkashanian, G.T. Rochelle, N. Shah, J.G. Yao, P.S. Fennell, Carbon capture and storage update, Energ. Environ. Sci. 7 (1) (2014) 130–189, doi:http://dx.doi.org/10.1039/C3EE42350F.
[8] J. Gibbins, H. Chalmers, Carbon capture and storage, Energy Policy 36 (12) (2008) 4317–4322, doi:http://dx.doi.org/10.1016/j.enpol.2008.09.058.
[9] A.J. Minchener, J.T. McMullan, Sustainable clean coal power generation within a European context—the view in 2006, Fuel 86 (14) (2007) 2124–2133, doi:http://dx.doi.org/10.1016/j.fuel.2007.01.022.
[10] A.-M. Cormos, C.-C. Cormos, Investigation of hydrogen and power co-generation based on direct coal chemical looping systems, Int. J. Hydrogen Energy 39 (5) (2014) 2067–2077, doi:http://dx.doi.org/10.1016/j.ijhydene.2013.11.123.
[11] C.-C. Cormos, Evaluation of syngas-based chemical looping applications for hydrogen and power co-generation with CCS, Int. J. Hydrogen Energy 37 (18) (2012) 13371–13386, doi:http://dx.doi.org/10.1016/j.ijhydene.2012.06.090.
[12] B. Erlach, M. Schmidt, G. Tsatsaronis, Comparison of carbon capture IGCC with pre-combustion decarbonisation and with chemical-looping combustion, Energy 36 (6) (2011) 3804–3815, doi:http://dx.doi.org/10.1016/j.energy.2010.08.038.
[13] L.-S. Fan, L. Zeng, W. Wang, S. Luo, Chemical looping processes for CO_2 capture and carbonaceous fuel conversion—prospect and opportunity, Energy Environ. Sci. 5 (6) (2012) 7254–7280, doi:http://dx.doi.org/10.1039/c2ee03198a.
[14] L.S. Fan, Chemical Looping Systems for Fossil Energy Conversions, Wiley, 2010.
[15] A. Lyngfelt, B. Leckner, T. Mattisson, A fluidized-bed combustion process with inherent CO_2 separation; application of chemical-looping combustion, Chem. Eng. Sci. 56 (10) (2001) 3101–3113, doi:http://dx.doi.org/10.1016/S0009-2509(01)00007-0.
[16] A. Tong, S. Bayham, M.V. Kathe, L. Zeng, S. Luo, L.-S. Fan, Iron-based syngas chemical looping process and coal-direct chemical looping process development at Ohio State University, Appl. Energy 113 (2014) 1836–1845, doi:http://dx.doi.org/10.1016/j.apenergy.2013.05.024.
[17] P. Casero, F.G. Peña, P. Coca, J. Trujillo, ELCOGAS 14 MWth pre-combustion carbon dioxide capture pilot. Technical & economical achievements, Fuel 116 (2014) 804–811, doi:http://dx.doi.org/10.1016/j.fuel.2013.07.027.
[18] P. Chiesa, S. Consonni, T. Kreutz, W. Robert, Co-production of hydrogen, electricity and CO from coal with commercially ready technology. Part A: performance and emissions, Int. J. Hydrogen Energy 30 (7) (2005) 747–767, doi:http://dx.doi.org/10.1016/j.ijhydene.2004.08.002.
[19] C. Kunze, H. Spliethoff, Assessment of oxy-fuel, pre- and post-combustion-based carbon capture for future IGCC plants, Appl. Energy 94 (2012) 109–116, doi:http://dx.doi.org/10.1016/j.apenergy.2012.01.013.
[20] Y. Oki, J. Inumaru, S. Hara, M. Kobayashi, H. Watanabe, S. Umemoto, H. Makino, Development of oxy-fuel IGCC system with CO_2 recirculation for CO_2 capture, Energy Procedia 4 (2011) 1066–1073, doi:http://dx.doi.org/10.1016/j.egypro.2011.01.156.
[21] C. Trapp, Advances in Model-Based Design of Flexible and Prompt Energy Systems—the CO2 Capture Plant at the Buggenum IGCC Power Station as a Test Case, Aerodynamics, Wind Energy, Flight Performance and Propulsion, University of Stuttgart, Netherlands, 2014.
[22] C. Kunze, H. Spliethoff, Modelling of an IGCC plant with carbon capture for 2020, Fuel Process. Technol. 91 (8) (2010) 934–941, doi:http://dx.doi.org/10.1016/j.fuproc.2010.02.017.
[23] C. Kunze, H. Spliethoff, Modelling, comparison and operation experiences of entrained flow gasifier, Energ. Convers. Manage. 52 (5) (2011) 2135–2141, doi:http://dx.doi.org/10.1016/j.enconman.2010.10.049.
[24] L. Zheng, E. Furinsky, Comparison of shell, Texaco, BGL and KRW gasifiers as part of IGCC plant computer simulations, Energy Convers. Manag. 46 (11–12) (2005) 1767–1779, doi:http://dx.doi.org/10.1016/j.enconman.2004.09.004.
[25] C.-C. Cormos, Evaluation of energy integration aspects for IGCC-based hydrogen and electricity co-production with carbon capture and storage, Int. J. Hydrogen Energy 35 (14) (2010) 7485–7497, doi:http://dx.doi.org/10.1016/j.ijhydene.2010.04.160.
[26] A. Brunetti, E. Drioli, G. Barbieri, Medium/high temperature water gas shift reaction in a Pd–Ag membrane reactor: an experimental investigation, RSC Adv. 2 (1) (2012) 226–233, doi:http://dx.doi.org/10.1039/C1RA00569C.
[27] M. Bracht, P.T. Alderliesten, R. Kloster, R. Pruschek, G. Haupt, E. Xue, J.R.H. Ross, M.K. Koukou, N. Papayannakos, Water gas shift membrane reactor for CO_2 control in IGCC systems: techno-economic feasibility study, Energy Convers. Manag. 38 (1997) S159–S164, doi:http://dx.doi.org/10.1016/S0196-8904(96)00263-4.
[28] C.-C. Cormos, Assessment of hydrogen and electricity co-production schemes based on gasification process with carbon capture and storage, Int. J. Hydrogen Energy 34 (15) (2009) 6065–6077, doi:http://dx.doi.org/10.1016/j.ijhydene.2009.05.054.
[29] J. Urech, L. Tock, T. Harkin, A. Hoadley, F. Maréchal, An assessment of different solvent-based capture technologies within an IGCC–CCS power plant, Energy 64 (2014) 268–276, doi:http://dx.doi.org/10.1016/j.energy.2013.10.081.

[30] F. Li, L. Zeng, L.G. Velazquez-Vargas, Z. Yoscovits, L.-S. Fan, Syngas chemical looping gasification process: bench-scale studies and reactor simulations, AIChE J. 56 (8) (2010) 2186–2199, doi:http://dx.doi.org/10.1002/aic.12093.

[31] P.-C. Chiu, Y. Ku, Chemical looping process—a novel technology for inherent CO$_2$ capture, Aerosol Air Qual. Res. 12 (2012) 1421–1432, doi:http://dx.doi.org/10.4209/aaqr.2012.08.0215.

[32] J. Adanez, A. Abad, F. Garcia-Labiano, P. Gayan, L.F. de Diego, Progress in chemical-looping combustion and reforming technologies, Prog. Energy Combust. Sci. 38 (2) (2012) 215–282, doi:http://dx.doi.org/10.1016/j.pecs.2011.09.001.

[33] S. Chen, W. Xiang, Z. Xue, X. Sun, Experimental investigation of chemical looping hydrogen generation using iron oxides in a batch fluidized bed, Proc. Combust. Inst. 33 (2) (2011) 2691–2699, doi:http://dx.doi.org/10.1016/j.proci.2010.08.010.

[34] R. Sharma, A. Delebarre, B. Alappat, Chemical-looping combustion—an overview and application of the recirculating fluidized bed reactor for improvement, Int. J. Energy Res. 38 (10) (2014) 1331–1350, doi:http://dx.doi.org/10.1002/er.3151.

[35] G. Azimi, M. Keller, A. Mehdipoor, H. Leion, Experimental evaluation and modeling of steam gasification and hydrogen inhibition in chemical-looping combustion with solid fuel, Int. J. Greenhouse Gas Control 11 (2012) 1–10, doi:http://dx.doi.org/10.1016/j.ijggc.2012.07.018.

[36] A. Cuadrat, A. Abad, L.F. de Diego, F. García-Labiano, P. Gayán, J. Adánez, Prompt considerations on the design of chemical-looping combustion of coal from experimental tests, Fuel 97 (2012) 219–232, doi:http://dx.doi.org/10.1016/j.fuel.2012.01.050.

[37] L.-S. Fan, Chemical Looping Systems for Fossil Energy Conversions, Wiley-AIChE, USA, 2010.

[38] L. Fan, F. Li, S. Ramkumar, Utilization of chemical looping strategy in coal gasification processes, Particuology 6 (3) (2008) 131–142, doi:http://dx.doi.org/10.1016/j.partic.2008.03.005.

[39] F. He, N. Galinsky, F. Li, Chemical looping gasification of solid fuels using bimetallic oxygen carrier particles—feasibility assessment and process simulations, Int. J. Hydrogen Energy 38 (19) (2013) 7839–7854, doi:http://dx.doi.org/10.1016/j.ijhydene.2013.04.054.

[40] T. Song, T. Shen, L. Shen, J. Xiao, H. Gu, S. Zhang, Evaluation of hematite oxygen carrier in chemical-looping combustion of coal, Fuel 104 (2013) 244–252, doi:http://dx.doi.org/10.1016/j.fuel.2012.09.030.

[41] B. Wang, H. Lv, H. Zhao, C. Zheng, Experimental and simulated investigation of chemical looping combustion of coal with Fe$_2$O$_3$ based oxygen carrier, Procedia Eng. 16 (2011) 390–395, doi:http://dx.doi.org/10.1016/j.proeng.2011.08.1100.

[42] L. Zeng, F. He, F. Li, L.-S. Fan, Coal-direct chemical looping gasification for hydrogen production: reactor modeling and process simulation, Energy Fuels 26 (6) (2012) 3680–3690, doi:http://dx.doi.org/10.1021/ef3003685.

[43] Aspentech, Physical Property Methods and Models, Aspen Physical Property System vol. 11, Aspentech, Cambridge, USA, 20011.

[44] Aspentech, Physical Property Methods, Aspen Physical Property System, Aspentech, Burlington, USA, 2010.

[45] T.J. Kotas, The Exergy Method of Thermal Plant Analysis, Anchor Brendon Ltd, Essex, England, 1985.

[46] A.P. Hinderink, F.P.J.M. Kerkhof, A.B.K. Lie, J. De Swaan Arons, H.J. Van Der Kooi, Exergy analysis with a flowsheeting simulator—I. Theory; calculating exergies of material streams, Chem. Eng. Sci. 51 (20) (1996) 4693–4700, doi:http://dx.doi.org/10.1016/0009-2509(96)00220-5.

[47] A. Aspelund, D.O. Berstad, T. Gundersen, An extended pinch analysis and design procedure utilizing pressure based exergy for subambient cooling, Appl. Therm. Eng. 27 (16) (2007) 2633–2649, doi:http://dx.doi.org/10.1016/j.applthermaleng.2007.04.017.

[48] I. Dincer, M.A. Rosen, Exergy: Energy, Environment and Sustainable Development, Elsevier, 2007.

[49] S. Harvey, N.D. Kane, Analysis of a reheat gas turbine cycle with chemical recuperation using aspen, Energ. Convers. Manage. 38 (15–17) (1997) 1671–1679, doi:http://dx.doi.org/10.1016/S0196-8904(96)00208-7.

[50] E. Querol, B. Gonzalez-Regueral, J.L. Perez-Benedito, Practical Approach to Exergy and Thermoeconomic Analyses of Industrial Processes, Springer, 2013.

[51] G.P. Verkhivker, B.V. Kosoy, On the exergy analysis of power plants, Energy Convers. Manag. 42 (18) (2001) 2053–2059, doi:http://dx.doi.org/10.1016/S0196-8904(00)00170-9.

[52] R.S. El-Emam, I. Dincer, G.F. Naterer, Energy and exergy analyses of an integrated SOFC and coal gasification system, Int. J. Hydrogen Energy 37 (2) (2012) 1689–1697, doi:http://dx.doi.org/10.1016/j.ijhydene.2011.09.139.

[53] H. Ozcan, I. Dincer, Thermodynamic analysis of a combined chemical looping-based trigeneration system, Energ. Convers. Manage. 85 (2014) 477–487, doi:http://dx.doi.org/10.1016/j.enconman.2014.06.011.

[54] I. Dincer, M.A. Rosen, Exergy: Energy, Environment and Sustainable Development, second edition, Elsevier, 2012.

[55] C.-C. Cormos, Evaluation of iron based chemical looping for hydrogen and electricity co-production by gasification process with carbon capture and storage, Int. J. Hydrogen Energy 35 (6) (2010) 2278–2289, doi:http://dx.doi.org/10.1016/j.ijhydene.2010.01.033.

[56] L.F. Pellegrini, S. de Oliveira Júnior, J.C. Burbano, Supercritical steam cycles and biomass integrated gasification combined cycles for sugarcane mills, Energy 35 (2) (2010) 1172–1180, doi:http://dx.doi.org/10.1016/j.energy.2009.06.011.

[57] J. Davison, Performance and costs of power plants with capture and storage of CO$_2$, Energy 32 (7) (2007) 1163–1176, doi:http://dx.doi.org/10.1016/j.energy.2006.07.039.

[58] IEA, CO2 Capture and Storage, International Energy Agency, 2008.

[59] M. Kanniche, R. Gros-Bonnivard, P. Jaud, J. Valle-Marcos, J.-M. Amann, C. Bouallou, Pre-combustion, post-combustion and oxy-combustion in thermal power plant for CO$_2$ capture, Appl. Therm. Eng. 30 (1) (2010) 53–62, doi:http://dx.doi.org/10.1016/j.applthermaleng.2009.05.005.

[60] A. Padurean, C.-C. Cormos, P.-S. Agachi, Pre-combustion carbon dioxide capture by gas–liquid absorption for integrated gasification combined cycle power plants, Int. J. Greenhouse Gas Control 7 (2012) 1–11, doi:http://dx.doi.org/10.1016/j.ijggc.2011.12.007.

[61] S. Rezvani, Y. Huang, D. McIlveen-Wright, N. Hewitt, J.D. Mondol, Comparative assessment of coal fired IGCC systems with CO$_2$ capture using physical absorption, membrane reactors and chemical looping, Fuel 88 (12) (2009) 2463–2472, doi:http://dx.doi.org/10.1016/j.fuel.2009.04.021.

[62] IEA, Cost and Performance of Carbon Dioxide Capture from Power Generation, International Energy Agency, 2011.

[63] T. Uchida, T. Goto, T. Yamada, T. Kiga, C. Spero, Oxyfuel combustion as CO$_2$ capture technology advancing for practical use—callide Oxyfuel Project, Energy Procedia 37 (2013) 1471–1479, doi:http://dx.doi.org/10.1016/j.egypro.2013.06.022.

[64] M. Anheden, G. Svedberg, Exergy analysis of chemical-looping combustion systems, Energy Convers. Manag. 39 (16–18) (1998) 1967–1980, doi:http://dx.doi.org/10.1016/S0196-8904(98)00052-1.

[65] N. Casas, J. Schell, L. Joss, M. Mazzotti, A parametric study of a PSA process for pre-combustion CO$_2$ capture, Sep. Purif. Technol. 104 (2013) 183–192, doi:http://dx.doi.org/10.1016/j.seppur.2012.11.018.

[66] Y. Li, Q. Fu, M. Flytzani-Stephanopoulos, Low-temperature water-gas shift reaction over Cu$^-$ and Ni-loaded cerium oxide catalysts, Appl. Catal. B Environ. 27 (3) (2000) 179–191, doi:http://dx.doi.org/10.1016/S0926-3373(00)00147-8.

[67] Y. Liu, Z.-S. Li, L. Xu, N. Cai, Effect of sorbent type on the sorption enhanced water gas shift process in a fluidized bed reactor, Ind. Eng. Chem. Res. 51 (37) (2012) 11989–11997, doi:http://dx.doi.org/10.1021/ie301100y.

[68] J. Schell, N. Casas, D. Marx, M. Mazzotti, Precombustion CO$_2$ capture by pressure swing adsorption (PSA): comparison of Laboratory PSA experiments and simulations, Ind. Eng. Chem. Res. 52 (24) (2013) 8311–8322, doi:http://dx.doi.org/10.1021/ie3026532.

[69] D.P. Hanak, C. Biliyok, H. Yeung, R. Białecki, Heat integration and exergy analysis for a supercritical high-ash coal-fired power plant integrated with a post-combustion carbon capture process, Fuel 134 (2014) 126–139, doi:http://dx.doi.org/10.1016/j.fuel.2014.05.036.

[70] IEA, CO$_2$ Emissions from Fuel Combustion, IEA, 2013.

[71] E. Querol, B. Gonzalez-Regueral, A. Ramos, J.L. Perez-Benedito, Novel application for exergy and thermoeconomic analysis of processes simulated with Aspen Plus®, Energy 36 (2) (2011) 964–974, doi:http://dx.doi.org/10.1016/j.energy.2010.12.013.

[72] T. Sanpasertparnich, R. Idem, I. Bolea, D. deMontigny, P. Tontiwachwuthikul, Integration of post-combustion capture and storage into a pulverized coal-fired power plant, Int. J. Greenhouse Gas Control 4 (3) (2010) 499–510, doi:http://dx.doi.org/10.1016/j.ijggc.2009.12.005.

[73] G. Xu, Y. Hu, B. Tang, Y. Yang, K. Zhang, W. Liu, Integration of the steam cycle and CO$_2$ capture process in a decarbonization power plant, Appl. Therm. Eng. 73 (1) (2014) 277–286, doi:http://dx.doi.org/10.1016/j.applthermaleng.2014.07.051.

[74] E. Jerndal, T. Mattisson, A. Lyngfelt, Thermal analysis of chemical-looping combustion, Chem. Eng. Res. Des. 84 (2006) 795–806.